This article was downloaded by:
On: *14 January 2011*
Access details: *Access Details: Free Access*
Publisher *Taylor & Francis*
Informa Ltd Registered in England and Wales Registered Number: 1072954 Registered office: Mortimer House, 37-41 Mortimer Street, London W1T 3JH, UK

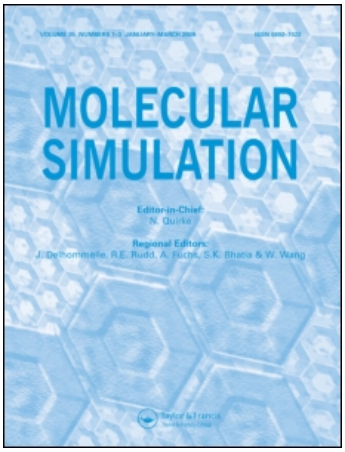

Molecular Simulation
Publication details, including instructions for authors and subscription information:
http://www.informaworld.com/smpp/title~content=t713644482

Simulated dynamics of $Ne@C_{60}$ aggregates beyond dissociation

P. Tilton[a]; B. Suchy[b]; M. K. Balasubramanya[a]; M. W. Roth[a]
[a] Department of Physical and Life Sciences, Texas A&M University, Corpus Christi, TX, USA [b] Department of Physics, University of Northern Iowa, Cedar Falls, IA, USA

Online publication date: 27 July 2010

To cite this Article Tilton, P. , Suchy, B. , Balasubramanya, M. K. and Roth, M. W.(2007) 'Simulated dynamics of $Ne@C_{60}$ aggregates beyond dissociation', Molecular Simulation, 33: 11, 945 — 952
To link to this Article: DOI: 10.1080/08927020701435803
URL: http://dx.doi.org/10.1080/08927020701435803

PLEASE SCROLL DOWN FOR ARTICLE

Full terms and conditions of use: http://www.informaworld.com/terms-and-conditions-of-access.pdf

This article may be used for research, teaching and private study purposes. Any substantial or systematic reproduction, re-distribution, re-selling, loan or sub-licensing, systematic supply or distribution in any form to anyone is expressly forbidden.

The publisher does not give any warranty express or implied or make any representation that the contents will be complete or accurate or up to date. The accuracy of any instructions, formulae and drug doses should be independently verified with primary sources. The publisher shall not be liable for any loss, actions, claims, proceedings, demand or costs or damages whatsoever or howsoever caused arising directly or indirectly in connection with or arising out of the use of this material.

Molecular Simulation, Vol. 33, No. 11, September 2007, 945–952

Taylor & Francis
Taylor & Francis Group

Simulated dynamics of Ne@C_{60} aggregates beyond dissociation

P. TILTON†, B. SUCHY‡, M. K. BALASUBRAMANYA† and M. W. ROTH‡*

†Department of Physical and Life Sciences, Texas A&M University, Corpus Christi, TX 78412, USA
‡Department of Physics, University of Northern Iowa, Cedar Falls, IA 50614, USA

(Received May 2006; in final form May 2007)

Molecular dynamics (MD) computer simulations are utilized to better understand the dynamics of small ($N = 5$) endohedral Ne@C_{60} aggregates. Multiple runs at various temperatures are used to increase the reliability of our statistics. The aggregate holds together until somewhere between $T = 1150$ and 1200 K, where it dissociates, showing no intermediate sign of melting or fullerene disintegration. When the temperature is increased to around $T = 4000$ K, the encapsulated neon atoms begin to leave the aggregate, with the fullerene molecules still remaining intact. At temperatures near $T = 4400$ K, thermal disintegration of the fullerenes preempts the aggregate dissociation. Above this temperature neon atoms are more quickly released and the fullerenes form a larger connected structure, with bonding taking place in atom pairs from different original fullerene molecules. Escape constants and half lives are calculated for the temperature range $4000\,\text{K} \leq T \leq 5000\,\text{K}$. The agreements and disagreements of results of this work with experiments suggest that classical MD simulations are useful in describing fullerene systems at low temperatures and near disintegration, but require development of new techniques before it is possible to accurately model windowing at temperatures below $T = 3000$ K.

Keywords: Endohedral fullerenes; Molecular dynamics; Noble gases; Encapsulation

Downloaded At: 17:47 14 January 2011

1. Introduction

For two decades, fullerenes have remained at the forefront of scientific curiosity and research efforts. They are physically interesting molecules in their own right and can display a rich diversity of behavior when they have atoms trapped inside their cages or have other atomic and molecular species adsorbed on their exterior. Because of their symmetry and durability it is of interest to place various atoms within a fullerene cage and study the dynamics of this endohedral system. Many experimental [1–14] and computational [15–28] studies address the behavior of endohedral fullerene/noble gas systems as well as the dynamics of fullerene systems and how they may encapsulate certain atoms. Encapsulation of noble gases by fullerenes happens frequently during the molecules' formation in the presence of noble gases at extraterrestrial sites and in the laboratory production processes employing an electric arc between carbon electrodes in a noble gas environment. Specifically, helium isotopes may be trapped in fullerenes found in extraterrestrial objects or even on the ancient earth and, if the sample size is large enough, unique helium isotope ratios are preserved and can, therefore, be calculated [29]. Study of such helium isotope ratios in endohedral fullerenes yields significant information about the extraterrestrial microscopic environment at the time of their formation.

Another interesting aspect of encapsulation is that for an aggregate of fullerene/endohedral noble gas molecules, the release of the encapsulated species can be studied as functions of temperature and time. Shimshi *et al.* [30] completed a mass spectroscopic study of the release of Ne@C_{60}. They found that it was possible for the fullerene to release a Ne atom without the molecular cage being destroyed, which is impossible if the Ne atom is simply pushed through the cage. Therefore, they attribute the release of the encapsulated species to a window mechanism [15,16]. Such a mechanism involves temporary carbon–carbon bond breaking which disrupts the hexagonal/pentagonal bond symmetry, opening the cage up for guest atom escape. After a guest atom has passed through the opening, the bond will re-form. They also find that, in the presence of impurities, the rate of release is increased by orders of magnitude. The half life for Ne escape at $T = 903$ K is more than one month but at $T = 1173$ K it is on the order of 10 h. Here, a modified window mechanism has been proposed, where the

*Corresponding author. Tel.: + 1-319-273-7336. Fax: + 1-319-273-7136. Email: rothm@uni.edu

Molecular Simulation
ISSN 0892-7022 print/ISSN 1029-0435 online © 2007 Taylor & Francis
http://www.tandf.co.uk/journals
DOI: 10.1080/08927020701435803

impurity (perhaps a radical) adds to the cage and weakens fullerene bonds and then leaves after the release, allowing reconstitution of the bonds. The fullerene bonding topology and the integrity of the bonding has a profound effect on the system's dynamics, as the introduction of an ambient gas [1,4], the introduction of bonding atoms [31] or even trace amounts of impurities [30] can dramatically affect the release rates, almost always promoting more rapid release and at lower temperatures. It is even possible to experimentally hold a fullerene window open so as to facilitate endohedral capture and release [13].

It is clear that much remains to be understood about the dynamics of small endohedral C_{60} aggregates that have broken off from a larger crystal, as well as the endohedral release process. Since classical MD simulations have had some success in aiding our understanding of the dynamics exhibited by fullerenes and fullerene complexes, it seems reasonable to extend such simulations to study the dynamics of endohedral noble gas–fullerene aggregates. We have chosen the noble gas for this study to be Ne. Specifically, the purpose of this study is to understand the dynamics of Ne@C_{60} aggregates better, to unravel the endohedral release process, and to determine half-lives for release. Classical MD simulations of many different fullerene systems have been completed [15–28], and it is well known that phase transition temperatures involving bonded interactions do not agree with experiment. Therefore, this study, while facilitating a better understanding of the results of other similar simulations [15–28] does not, and cannot be expected to, provide phase transition temperatures that fit experimental results.

Downloaded At: 17:47 14 January 2011

2. Computational approach

The Ne@C_{60} aggregate chosen for this study has five endohedral fullerenes. Previous work has been done on the stability of fullerene aggregates with up to 25 members [32]. In our simulations, we picked an aggregate size that was not particularly biased for stability or instability. In addition, we wanted to use the smallest such aggregate because the process of release takes a substantial amount of simulated time. With a smaller aggregate size, it is possible to do many runs and obtain reasonable statistics. Based on the plots resulting from experimental work [32], the aggregate size we chose had $N = 5$. Moreover, in a real aggregate containing many more fullerenes, as the temperature rises, smaller crystallites leave the aggregate edge and it is likely that endohedral release happens in the gas phase from such small free crystallites. For this reason, periodic boundary conditions are not utilized; we wish to simulate small aggregates where edge effects are important and aggregate dissociation is not stifled. There is a very large reflecting box the aggregate is kept in so that the system volume is constant. However, none of the particles ever reflect off this wall in our simulation, so in actuality we implement free boundary conditions on the aggregate. Above 257 K, the fullerite crystal forms an FCC lattice. As shown in figure 1, we model the initial configuration of the aggregate at every temperature as one face of an FCC unit cell which has sheared off from the cell. To simulate the Ne@C_{60} complexes an (N,V,T) MD method is utilized.

As simulated time runs forward, the equations of motion are integrated using a standard Verlet algorithm with a time step $\Delta t = 0.0005$ ps, and various thermodynamic quantities and order parameters of interest are calculated. At each of the temperatures $T = 1000$, 2000, 3000, 4000, 5000 K, 100 runs are completed, with initial velocities being randomized so that a robust statistical picture of release can emerge from this study. In the temperature ranges $1000\,\mathrm{K} \leq T \leq 2000\,\mathrm{K}$ and $4000\,\mathrm{K} \leq T \leq 5000\,\mathrm{K}$, the results of five different runs were averaged at temperatures spaced 50 K apart. The former range addresses aggregate dissociation and the latter focuses on individual fullerene disintegration. Temperature control is achieved by velocity rescaling for the carbon atoms in fullerene and the noble gas population separately. Each run is taken out to 2×10^6 time steps (1 ns) by which time equilibration is attained. In our simulation we average the time it takes the first trapped Ne atom to escape from the aggregate of cages at every temperature considered. At $T = 4000$ K the average escape time is less than 1 ns with a standard deviation on the order of a few hundred picoseconds.

There are several types of interaction potentials used in the simulations. The neon–neon potential as well as the

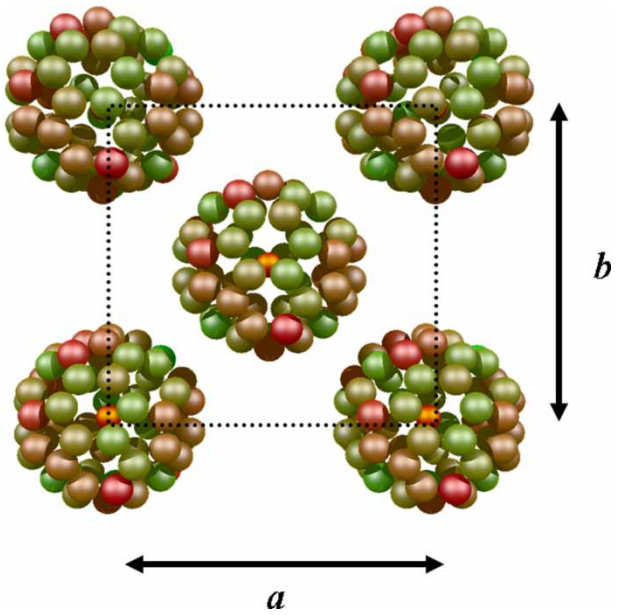

Figure 1. Initial conditions utilized for the simulations. The five fullerenes in the aggregate form one face of an FCC fullerite unit cell with lattice constants $a = b = 14.4$ Å. The carbon atoms in each fullerene are colored green if they are closest to its center of mass, red if they are farthest away and a mixture of red and green if they are in between. The orange atoms inside the fullerene cages are encapsulated Ne atoms, and the relative atomic sizes, chosen for visual clarity, are not to scale.

Downloaded At: 17:47 14 January 2011

neon–carbon potential are of a Lennard–Jones form,

$$u_{\mathrm{LJ}}(r_{ij}) = 4\varepsilon_{ij}\left[\left(\frac{\sigma_{ij}}{r_{ij}}\right)^{12} - \left(\frac{\sigma_{ij}}{r_{ij}}\right)^{6}\right], \tag{1}$$

where the potential parameters between various species are given in table 1; mixed interaction parameters are obtained with the use of Lorentz–Bertholot combining rules involving C—C parameters for the same potential as in equation (1). The r_{ij}^{-12} term results in a repulsive force that becomes strongly evident when electron clouds of interacting atoms overlap. Ultimately, such repulsion has its origin in the Pauli exclusion principle. The r_{ij}^{-6} dispersion term has its origin in the van der Waals attractive forces arising from fluctuating dipolar interactions. In addition, there is a non-bonded carbon–carbon interaction [27] which is in a *modified* Lennard–Jones form

$$u_{\mathrm{LJ}}(r_{ij}) = \varepsilon_{\mathrm{CC}}\left[\left(\frac{\sigma_{\mathrm{CC}}}{r_{ij}}\right)^{12} - 2\left(\frac{\sigma_{\mathrm{CC}}}{r_{ij}}\right)^{6}\right] \tag{2}$$

whose parameters are also shown in table 1. The carbon–carbon bonded interactions are modeled by Brenner's empirical extended bond-order potential [33] which has parameters that are fit to various energetics of hydrocarbons, diamond and graphite.

$$\left.\begin{aligned} V_{\mathrm{R}}(r_{ij}) &= f(r_{ij})\tfrac{D_e}{S-1}\exp[-\beta\sqrt{2S}(r-R_e)] \\ V_{\mathrm{A}}(r_{ij}) &= f(r_{ij})\tfrac{D_e S}{S-1}\exp\left[-\beta\sqrt{\tfrac{2}{S}}(r-R_e)\right] \\ f(r_{ij}) &= \begin{cases} 1, & r < R_1 \\ \frac{1}{2}\left[1+\cos\left(\frac{(r_{ij}-R_1)\pi}{(R_2-R_1)}\right)\right], & R_1 < r_{ij} < R_2 \\ 0, & r_{ij} > R_2 \end{cases} \end{aligned}\right\}, \tag{3a}$$

In equations (3a), V_{R} and V_{A} are the repulsive and attractive terms, respectively, which are essentially modified Morse potentials. The screening function $f(r_{ij})$ restricts the interaction to nearest neighbors as defined by the values for R_1 and R_2. In addition, the Brenner potential takes bonding topology into account with the empirical bond order function $\bar{B}_{ij}$ given by the relationships

$$\left.\begin{aligned} B_{ij} &= 1 + \left[\textstyle\sum_{k\neq i,j}^{N} G_C(\theta_{ijk}) f(r_{ik})\right]^{-\delta} \\ G_C(\theta) &= a_0\left[1 + \tfrac{c_0^2}{d_0^2} - \tfrac{c_0^2}{d_0^2 + (1+\cos\theta)^2}\right] \\ \bar{B}_{ij} &= \tfrac{B_{ij}+B_{ji}}{2} \end{aligned}\right\}. \tag{3b}$$

Here, the three-body bond angle is defined as

$$\theta_{ijk} = \cos^{-1}\left(\frac{\vec{r}_{ji}\cdot\vec{r}_{jk}}{r_{ji}\,r_{jk}}\right), \tag{3c}$$

where $\vec{r}_{ab}$ is the displacement vector from carbon atom a to carbon atom b. Variations of the Brenner potential have been used for many different types of carbon allotrope simulations, as the empirical bond order function controls aggregate formation to some extent. For example, Yamaguchi *et al.* [22–26] do not include information from the conjugate compensation term [33] because with it the potential would not adequately apply to small aggregates having non-terminated carbons. Since we are dealing initially with complete fullerenes which eventually break up, we disregard the compensation term as well. The entire carbon–carbon interaction is a sum over all bonded and non-bonded interactions:

$$u_{\mathrm{CC}} = \sum_{i=1}^{N}\sum_{j>i}^{N}\{[V_{\mathrm{R}}(r_{ij}) - \bar{B}_{ij}V_{\mathrm{A}}(r_{ij})] + P_{ij}u_{\mathrm{LJ}}(r_{ij})\}. \tag{4}$$

Here, P_{ij} is a screening function [27] which we implement by creating bonded and non-bonded neighbor lists. All carbon–carbon bonded potential parameters are given in table 2.

3. Results and discussion

At low temperature ($T = 1000\,\mathrm{K}$) the aggregate holds together, as do the fullerene molecules comprising it. This is evidenced for the aggregate by the sharp peak in the inter-fullerene pair distribution function $P_{\mathrm{inter}}(r_{ij})$ shown in figure 2, which is the calculated frequency of occurrence of a certain carbon atom pair separation between two carbon atoms in different fullerenes being

Table 1. Parameters for the non-bonded Lennard–Jones interaction potentials.

Species	ε_{ij}*(K)*	σ_{ij} *(Å)*
Ne—Ne	36.68	2.79
C—C*	28.00*	3.40*
C—C	34.839	3.805

The interactions with asterisks (*) in the middle row are not used explicitly in the simulations because they are for a standard LJ interaction, not the modified one actually used. Rather, they are used only in combining rule relationships to get Ne–C interactions of the form in equation (1).

Table 2. Parameters for the bonded carbon–carbon Brenner interaction potential.

Parameter	*Value*
D_e	73333.33 K
β	1.5 Å^{-1}
S	1.29
R_e	1.315 Å
R_1	1.7 Å
R_2	2.000 Å
δ	0.80469
a_0	0.011304
c_0	19
D_0	2.5

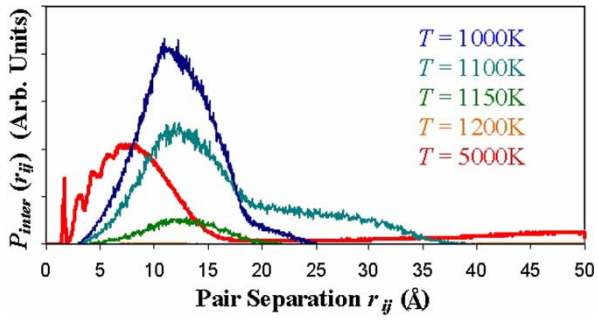

Figure 2. Inter-fullerene pair distribution function $P_{\text{inter}}(r_{ij})$ for temperatures $T = 1000$ K (blue), 1100 K (cyan), 1150 K (green), 1200 K (orange; barely visible on the horizontal axis) and 5000 K (red).

between r_{ij} and $r_{ij} + \Delta r_{ij}$, divided by the normalizing factor $2\pi r_{ij}\Delta r_{ij}$.

The low-temperature structure in the fullerenes themselves is quantified in a few different ways. Figure 3 shows a sharp low-temperature peak in $P(r)$, the fullerene radial probability distribution, which is the calculated probability of a carbon atom being a certain distance from the center of mass of the fullerene molecule containing it. Moreover, the low-temperature fullerene pair distribution function $P_f(r_{ij})$ shown in figure 4 exhibits a strong solid-like signature. $P_f(r_{ij})$ is calculated exactly as $P_{\text{inter}}(r_{ij})$ is,

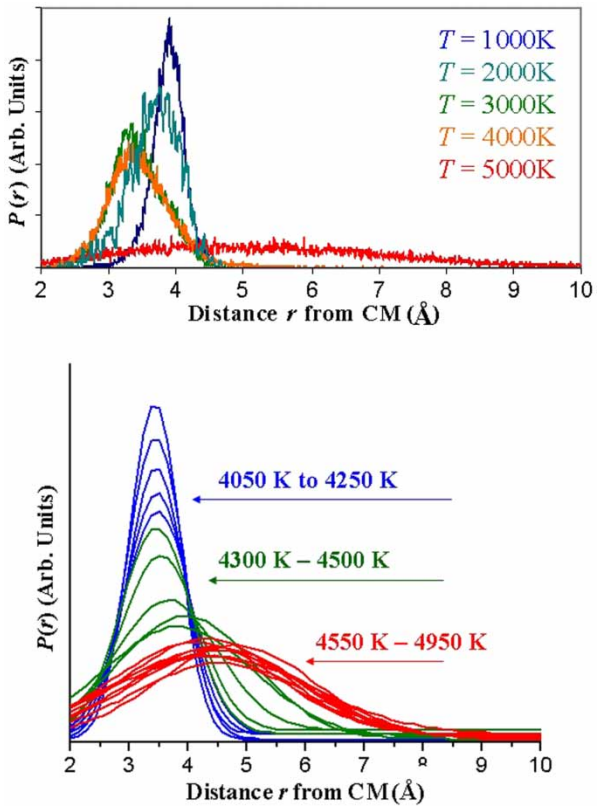

Figure 3. Top: $P(r)$, the fullerene radial probability distribution for $T = 1000$ K (blue), 2000 K (cyan), 3000 K (green), 4000 K (orange) and 5000 K (red). Bottom: Best Gaussian fits for 4050 K $\leq T \leq$ 4950 K split into blue, green and red groups as indicated on the plot. The Gaussian fits are chosen for visualization ease because of the number of curves present, and the fastest change in their character take place between $T = 4300$ and 4500 K, corresponding to the green group of curves.

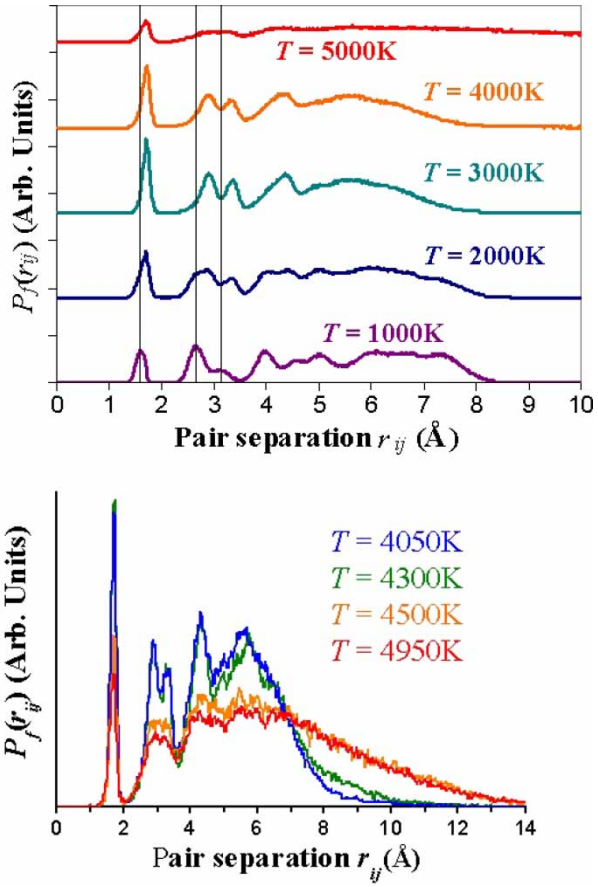

Figure 4. Top: fullerene pair distribution function $P_f(r_{ij})$ for $T = 1000$ K (purple), 2000 K (blue), 3000 K (cyan), 4000 K (orange) and 5000 K (red). Bottom: fullerene pair distribution function $P_f(r_{ij})$ for $T = 4050$ K (blue), 4300 K (green), 4500 K (orange) and 4950 K (red). In the upper plot, vertical lines indicate the location of the low-temperature peaks for first, second and third neighbors. In the lower plot, note that there is a large change in the character of the curves between $T = 4300$ and 4500 K.

with the exception that both carbon atoms in the pairs are in the same fullerene molecule.

Inspection of $P_{\text{inter}}(r_{ij})$ in figure 2 gives an indication of the first significant change in the system with increasing temperature. As the temperature increases from $T = 1000$ K, the peak near $r_{ij} = 12$ Å dramatically drops in amplitude due to thermal fluctuations. By $T = 1200$ K the distribution is essentially flat, because all the atom pair separations are greater than the highest value of the abscissa of the plot. Therefore, the data suggests that the aggregate dissociates in the temperature range 1150 K $\leq T \leq$ 1200 K, which is in agreement with other calculations [34,35] of the melting of C_{60} structures under pressure, and the well known fact that, at low pressure, fullerites sublime and do not melt. The plots of $P_f(r_{ij})$ in figure 4 illustrate that the dissociation of the aggregate has no noticeable general effect on the structure of the fullerene molecules themselves. However, the plateau between $r_{ij} = 6$ and 7.5 Å present at low temperature dies off more quickly at higher temperatures, suggesting that the walls of the molecules themselves become slightly thinner with increasing temperature. The plots of $P(r)$ in

Downloaded At: 17:47 14 January 2011

Downloaded At: 17:47 14 January 2011

figure 3 confirm the insensitivity of the fullerene molecules to the aggregate dissociation and also show that in the temperature range $1050\,\mathrm{K} \leq T \leq 1950\,\mathrm{K}$ the peak in the distributions actually shifts towards lower distances, which suggests that as temperature increases from $T = 1000\,\mathrm{K}$ the molecules also contract slightly. Negative thermal expansion coefficients in this temperature range have recently been observed experimentally [36]. Typical molecular snapshots shown in figure 5 confirm that the aggregate holds together until around $T = 1150\,\mathrm{K}$ and then dissociates with the endohedral fullerenes still intact.

As the temperature is raised beyond $T = 2000\,\mathrm{K}$, the endohedral fullerenes show expected signs of thermal fluctuation, with very little change between $T = 3000$ and 4000 K, and the molecular cages still remaining intact. This is evidenced in part by the profound solid-like character for the system still present in the distributions at $T = 4000$ shown in figures 3 and 4. In addition, the thermal average of the system's total configurational energy $\langle U_c \rangle$ (T) shown in figure 6 does not exhibit a sharp increase, showing the absence of a proliferation in carbon–carbon bond breaking which would be present for molecular disintegration. Moreover, the average maximum and minimum moments of inertia ($I_{\max}$ and $I_{\min}$, respectively, shown in figure 7) are calculated by

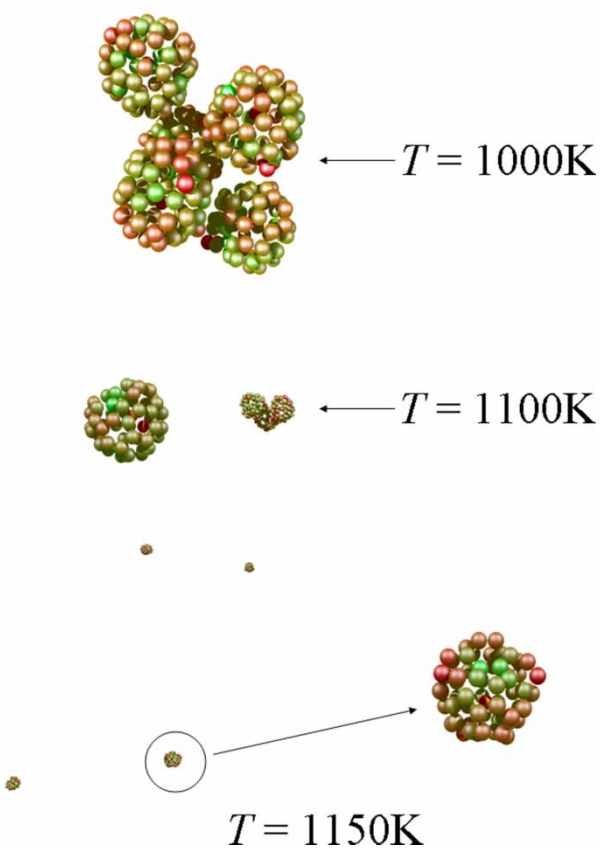

Figure 5. Final typical snapshots of the system from low temperature through aggregate dissociation. The color scheme is identical to that in figure 1.

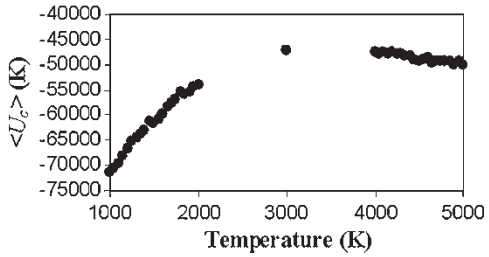

Figure 6. Thermal average of the system's total configurational energy, $\langle U_c \rangle(T)$.

obtaining the maximum and minimum eigenvalues of the inertia tensor for each molecule and averaging them over all the runs at a given temperature. As expected the two extreme moments of inertia become slightly higher as temperature increases. The difference ΔI between the two extreme moments of inertia (a quantitative measure of the degree of oblateness of the fullerenes) increases with temperature but does not show any sharp changes at or below $T = 4000\,\mathrm{K}$, confirming that the fullerene molecules remain intact up to this temperature.

At $T \approx 4000\,\mathrm{K}$, the first endohedral neon atoms are released from the aggregate. Our simulations show that windows form and close at the onset of release but somewhere before $T = 5000\,\mathrm{K}$ they become permanent defects in the fullerene cage. In previous work [28], we simulated the dynamics of single endohedral fullerenes as well as empty fullerene cages. Encapsulated species include noble gases up to $X@C_{60}$ with X = He, Ne, Ar, Kr and Xe. It was found that an encapsulated He atom disrupted the cage relative to the empty cage but larger encapsulated species tended to stabilize the cage slightly. Although we reported temperatures in that paper for which the fullerene cage held together, the same trend holds true for windowing and disintegration for this system. Current work [37] regarding endohedral release for various encapsulated noble gases confirms our previous work at temperatures below disintegration [28]. We find that larger endohedral species are released at slower rates, and helium release happens unusually rapidly. Typical results are as follows. Near $T = 4000\,\mathrm{K}$ windows form and then shut. At about $T = 4200\,\mathrm{K}$ permanent windows form and then near

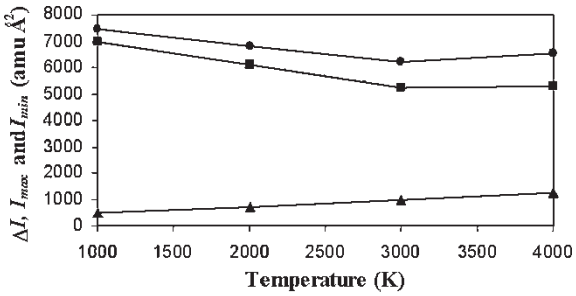

Figure 7. Maximum (circles) and minimum (squares) moments of inertia $I_{\max}$ and $I_{\min}$, respectively, for the fullerene molecules, and the difference ΔI between the two extreme inertia values (triangles).

$T = 4500$ K there is some unfolding present in the fullerene cage which results in large windows. Smaller endohedral species cause more destructive windowing at lower temperatures (on the order of a few hundred Kelvin between He and Xe), promoting earlier and more frequent release.

As the temperature increases, atom release begins sooner and happens more rapidly. This is evidenced in part by figure 8, showing t_1, the time of release for the first Ne atom in the aggregate, starting from the entrapped state in the aggregate at the beginning of the simulation, as a function of temperature. In addition, the number of Ne atoms encapsulated within the aggregate as functions of time for each temperature is fit to curves of the form

$$N(t, T) = N_0 e^{-k(T)t}, \tag{5}$$

and the rate constants $k(T)$ as functions of temperature are shown in figure 9. Selected release half lives as calculated from the rate constants are shown in table 3. As the temperature increases past $T = 4000$ K, $P(r)$ in figure 3 and $P_f(r_{ij})$ in figure 4 show that the fullerenes themselves are losing structural order. The curves for the finer temperature scale ($4050\text{ K} \leq T \leq 4950$ K) in figure 3 and the bottom plot in figure 4 both show that the fullerenes lose a considerable amount of structural order vis-à-vis the radial atomic distribution distance as well as the pair distribution function, respectively, near $T = 4400$ K. Since this is when the moments of inertia begin to grow very large (well off the scale of the plot) but the configurational energy does not, the loss of structural order here is interpreted to be from disintegration and recombination. Specifically, the individual fullerene cages begin to dissociate into carbon multimers. Then the resulting multimers which are sufficiently near to others combine to form larger carbon aggregates. This recombination is a result of starting with the fullerenes close together as an aggregate in the form of one face of the FCC unit cell and would not result from starting the simulation with a disordered aggregate of fullerenes. The temperature at which the fullerenes themselves show this profound loss of structural order is in excellent agreement with disintegration temperatures obtained by other MD calculations involving C_{60} [19] although it is well known that they differ from experimental values. In addition, between $T = 4000$ and 4300 K our simulations show that dynamic windowing (windows that open and close) is taking place, but at higher temperatures the windowing results in *permanent disorder being imparted to the fullerene* as discussed above. In our simulations dynamic windowing is evident by careful inspection of snapshots (shown and discussed later) as well as bond angle distributions (not shown, as we are interested in the aggregate dynamics and not the windowing mechanism in particular). In contrast, permanent windowing above $T = 4300$ K is shown again by inspection of snapshots but also by the sharp drop in the height of first peak of the pair distribution function shown in the bottom of figure 3. Hence, our simulations strongly support the idea that impurities catalyze some windowing mechanism in the fullerene. The presence of recombination is also confirmed by the $P_{\text{inter}}(r_{ij})$ curve at $T = 5000$ K in figure 2, where there is a sharp peak near 1.5 Å indicating that bonding *between atoms from different fullerenes* has taken place. The series of broader peaks at higher separations shows that atoms from different fullerenes have merged to create other bonded structures. Typical molecular snapshots shown in figure 10 illustrate and confirm the onset of endohedral release near $T = 4000$ K, the profound loss of structural order of the fullerene cage between $T = 4300$ and 4500 K and the contraction of the molecules as temperature increases from $T = 1000$ K up to $T = 3000$ K as well as recombination at the highest temperatures studied here. Also, the lack of windows for $T < 4300$ K is evidence that dynamic windowing is taking place to facilitate release but permanent windows are visible at

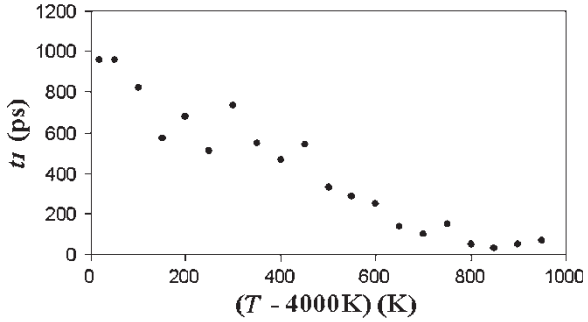

Figure 8. Time t_1 of first atom release as a function of temperature. The abscissa is offset by 4000 K in order be consistent with that of figure 7.

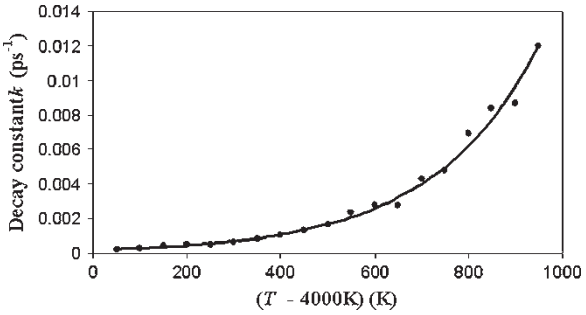

Figure 9. Rate constants $k(T)$ as functions of temperature. The solid line is the best exponential fit to the data (for visual aid) and the abscissa is offset by 4000 K in order to facilitate curve fitting.

Table 3. Half lives $t_{1/2}$ for endohedral escape for Ne and, in the bottom row (∗), for He.

Temperature (K)	$t_{1/2}$	*Source*
4050	2.97 ns	This work
4500	0.41 ns	This work
4950	0.057 ns	This work
903	6.1 yr	[30]
1173	57.8 h	[30]
293∗	40.3 h∗	[13]∗

Downloaded At: 17:47 14 January 2011

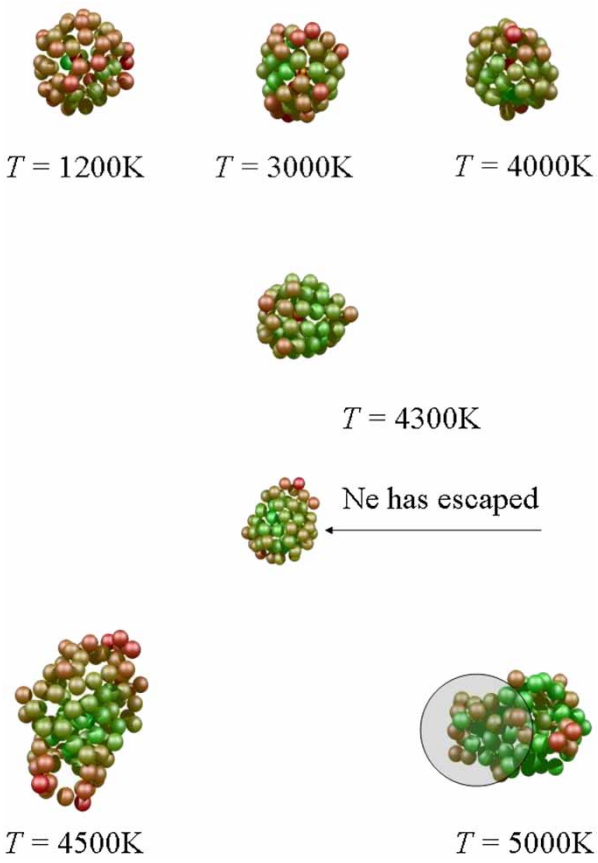

Figure 10. Final typical snapshots of the system past the dissociation temperature up through endohedral release, and ultimately high temperature recombination, of carbon atoms from different fullerenes. Individual fullerenes are shown, although two molecules in an aggregate happen to be shown together at $T = 4300$ K and the Ne atom has escaped from the bottom fullerene. Note the contraction of the molecule between $T = 1200$ and 3000 K and the substantial loss of order between $T = 4300$ and 4500 K. In addition, the atoms circled in the lower right were in a different fullerene at the start of the simulation. They have bunched with carbon atoms of the disintegrated fullerene shown. The color scheme is identical to that in figure 1.

higher temperatures. Moreover, inspection of the structures shown in figure 10 at high temperature indeed confirms that, since the fullerenes themselves exhibit disorder before the aggregate has time to dissociate, recombination can occur.

The $Ne@C_{60}$ dissociation temperature, as well as the temperature of thermal disintegration of our fullerene molecules, is in good agreement with previous calculations [19,33,34]. Although we are unable to locate any prior simulation studies of endohedral noble gas atom release, the results obtained in this study differ considerably from that obtained experimentally [30] and some discussion follows. In previous work [28], we simulated the dynamics of empty fullerenes. While we reported data in that paper in the temperature range where the fullerene held together we also obtained windowing and disintegration at temperatures similar to those obtained by other simulations (but different from experiment). Although the bonded potential used here can help elucidate some aspects of the bonded dynamics in nanoscale systems it does not describe the bonded character accurately enough to give transition temperatures that agree with experiment. *No technique currently exists that predict these transition temperatures*. Such inadequacy is well known but the potential has still been widely used for nanotube and fullerene systems to profitably study their dynamics. Our simulations in this work are conducted with no species of any kind surrounding the fullerenes, and the only way bonds can be broken is with thermal agitation—i.e. the character of the C–C bonds are not being altered. This is in contrast to other simulations where higher energy noble gas atoms collide with the fullerene structure, causing a window which then closes [15,16]. In real experiments, there are other atoms/molecules surrounding the system, and bond breaking/forming has been shown to be extremely sensitive to any species that may attempt to bond with the fullerene, and the effect is almost always to accelerate release. It is likely that, in the real molecule, the outer electrons of noble gas atoms encapsulated within the fullerenes interact dynamically with the fullerene bonds. In fact, when a window is held open in a fullerene, ^{3}He escape half lives at $T = 333$ K are already as low as 1.4 h. In our study, then, a picture emerges where the simulation results seem generally reasonable at (1) low temperatures where non-bonded Lennard–Jones interactions dominate phase transitions, and (2) near thermal disintegration of fullerenes. Hence, in the temperature range $4000\ \text{K} \leq T \leq 5000\ \text{K}$, it is reasonable to assume that the windowing suspected of causing the Ne release seen in experiment [30] would not have nearly the effect that thermal windowing seen in our simulations does. However, in order to accurately deal with thermal windowing and model escape at temperatures well below those for thermal disintegration of fullerenes, two challenges arise immediately. To begin with, a temperature-dependent description of the bond integrity as affected by any exohedral species will be required. That is, the simulations should somehow take into account the effect of impurities on any windowing mechanisms. Moreover, the escape process will have to be artificially accelerated in such a way as to preserve the integrity of the physics of the model, because in order for the endohedral population to become half of its initial value, the simulation will have to run for one half life which, even taking an underestimate of $t_{1/2} = 10$ h, would require 7.2×10^{19} steps using a time step of 0.0005 ps, translating to a real time commitment (in the case of this study) of more than the currently accepted value for the age of the universe.

We emphasize that the conclusions reached from this work apply only to small C_{60} aggregates, and most closely with those which are sheared off from a fullerite FCC cell in its equilibrium configuration. Studies such as simulations of endohedral fullerene aggregates of varying size, to characterize the importance of the interior of the system to the noble gas release, and also incorporating the effect of the aggregate becoming more crystalline, would be interesting extensions of this work.

Downloaded At: 17:47 14 January 2011

Acknowledgements

The authors are indebted to David Tomanek for candid discussions regarding this work. M.W.R acknowledges useful discussions with J. Che and R.J. Cross, as well as a UNI student fellowship for B.S. during the summer of 2004. M.K.B. acknowledges support for molecular dynamics simulations by the MRI program of the US National Science Foundation's Division of Computer and Network Systems, under grant numbered 0321218.

References

[1] M. Saunders, R.J. Cross. Putting nonmetals into fullerenes. *Endofullerenes*, Kluwer, Dordrecht (2002).
[2] M. Saunders, R.J. Cross, H.A. Jiménez-Vázquez, R. Shimshi, A. Khong. Noble gas atoms inside fullerenes. *Science*, **271**, 693 (1996).
[3] M.S. Syamala, R.J. Cross, M. Saunders. ^{129}Xe NMR spectrum of xenon inside C_{60}. *J. Am. Chem. Soc.*, **124**, 6216 (2002).
[4] R.J. Cross, A. Khong, M. Saunders. Using cyanide to put noble gases inside C_{60}. *J. Org. Chem.*, **68**(21), 8281 (2003).
[5] T. Sternfeld, R.E. Hoffman, M. Saunders, R.J. Cross, M.S. Syamala, M. Rabinovitz. Two helium atoms inside fullerenes: probing the internal magnetic field in C_{60}^{6-} and C_{70}^{6-}. *J. Am. Chem. Soc.*, **124**, 8786 (2002).
[6] J. Laskin, T. Peres, C. Lifshitz, M. Saunders, R.J. Cross, A. Khong. An artificial molecule of Ne_2 inside C_{70}. *Chem. Phys. Lett.*, **285**, 7 (1998).
[7] T. Weiske, H. Schwarz, D.E. Giblin, M.L. Gross. High-energy collisions of $Kr@C_{60}^{+}$ with helium: evidence for the formation of $HeKr@C_{60}^{+}$. *Chem. Phys. Lett.*, **227**, 87 (1994).
[8] Y. Rubin, T. Jarrosson, G.W. Wang, M.D. Bartberger, M.N. Houk, G. Schick, *et al.* Insertion of helium and molecular hydrogen through the orifice of an open fullerene. *Angew. Chem. Int. Ed. Engl.*, **40**, 1543 (2001).
[9] T. Peres, B.P. Cao, W.D. Cui, A. Khong, R.J. Cross, M. Saunders, C. Lifshitz. Some new diatomic molecules containing endohedral fullerenes. *Int. J. Mass Sprectrom.*, **210/211**, 241 (2001).
[10] T. Suetsuna, N. Dragoe, H. Shimotani, A. Takada, S. Ito, R.J. Cross, *et al.* Chromatographic purification of $Kr@C_{60}$. *Fullerene. Nanot. Carbon Nanostruct.*, **10**, 15 (2002).
[11] H.M. Lee, M.M. Olmstead, T. Suetsuna, H. Shimotani, N. Dragoe, R.J. Cross, *et al.* Crystallographic characterization of $Kr@C_{60}$ in $(0.09Kr@C_{60}/0.91C_{60})\cdot\{NiII(OEP)\}\cdot 2C_6H_6$. *Chem. Commun.*, 1352 (2002).
[12] S. Ito, A. Takeda, T. Miyazaki, Y. Yokoyama, M. Saunders, R.J. Cross, *et al.* Kr extended X-ray absorption fine structure study of endohedral $Kr@C_{60}$. *J. Phys. Chem. B*, **108**, 3191 (2004).
[13] C.M. Stanisky, R.J. Cross, M. Saunders, M. Murata, Y. Murata, K. Komatsu. Helium entry and escape through a chemically opened window in a fullerene. *J. Am. Chem. Soc.*, **127**, 299 (2005).
[14] R.J. Cross, M. Saunders. Transmutation of fullerenes. *J. Am. Chem. Soc.*, **127**(9), 3044 (2005).
[15] E. Sanville, J.J. DelBruno. Computational studies of possible transition structures in the insertion and windowing mechanisms for the formation of endohedral fullerenes. *J. Phys. Chem B*, **107**, 8884 (2003).
[16] S. Patchkovskii, W. Thiel. How does helium get into buckministerfullerene? *J. Am. Chem. Soc.*, **118**, 7164 (1996).
[17] T.H. Feng, W.J. Chang. Phase transformations of fullerenes using molecular dynamics simulations. *Microelectron. J.*, **35**, 581 (2004).
[18] S.G. Kim, D. Tomanek. Melting the fullerenes: a molecular dynamics study. *Phys. Rev. Lett.*, **72**(15), 2418 (1994).
[19] B.L. Zhang, C.Z. Wang, C.T. Chan, K.M. Ho. Thermal disintegration of carbon fullerenes. *Phys. Rev. B*, **48**(15), 11381 (1993).
[20] R.T. Chancey, L. Oddershede, F.E. Harris, J.R. Sabin. Fragmentation of fullerenes. *Phys. Rev. A*, **67**, 43203 (2003).
[21] A. Martinez-Alonso, J.M.D. Tascon, E.J. Bottani. Physical adsorption of Ar and CO_2 on C_{60} fullerene. *J. Phys. Chem. B*, **105**, 135 (2001).
[22] Y. Yamaguchi, S. Maruyama. A molecular dynamics study on the formation of metallofullerene. *Eur. Phys. J.*, **9**(1–4), 385 (1999).
[23] S. Maruyama, Y. Yamaguchi. A molecular dynamics of the formation process of fullerene. *Trans. JSME, Ser. B*, **63–611**, 2405 (1997).
[24] Y. Yamaguchi, S. Maruyama. A molecular dynamics simulation of the fullerene formation process. *Chem. Phys. Lett.*, **286**, 336 (1998).
[25] S. Maruyama, Y. Yamaguchi. A molecular dynamics demonstration of annealing to a perfect C_{60} structure. *Chem. Phys. Lett.*, **286**, 343 (1998).
[26] Y. Yamaguchi, S. Maruyama. A molecular dynamics of the formation process of fullerene. *Trans. JSME, Ser. B*, **63–611**, 2398 (1997).
[27] J. Che, T. Çagin, W.A. Goddard. Studies of fullerenes and carbon nanotubes by an extended bond order potential. *Nanotechnology*, **10**, 263 (1999).
[28] W. Even, J. Smith, M.W. Roth. Molecular dynamics simulations of noble gases encapsulated in C_{60} fullerene. *Mol. Simul.*, **31**(4), 207 (2005).
[29] L. Becker, R.J. Poreda, T.E. Bunch. Fullerenes: an extraterrestrial carbon carrier phase for noble gases. *Proc. Natl. Acad. Sci.*, **97**(7), 2979 (2000).
[30] R. Shimshi, A. Khong, H.A. Jimenez-Vasquez, R.J. Cross, M. Saunders. Release of noble gas atoms from inside fullerenes. *Tetrahedron*, **52**(14), 5143 (1996).
[31] M. Waiblinger, K. Lips, W. Harneit, A. Weidinger, E. Dietel, A. Hirsch. Thermal stability of the endohedral fullerenes $N@C_{60}$, $N@C_{70}$, and $P@C_{60}$. *Phys. Rev. B*, **63**, 45421 (2001).
[32] C. Rey, L.J. Gallego, J.A. Alonso. Molecular-dynamics study of the structure, binding energy, and melting of small clusters of fullerene molecules using Girifalco's spherical model. *Phys. Rev. B*, **49**, 8491 (1994).
[33] D.W. Brenner. Empirical potential for hydrocarbons for use in simulating the chemical vapor deposition of diamond films. *Phys. Rev. B*, **42**(15), 9458 (1990).
[34] M.C. Abramo, C. Caccamo, D. Costa, G. Pellicane, R. Ruberto. Atomistic versus two-body central potential models of C_{60}: a comparative molecular dynamics study. *Phys. Rev. E*, **69**, 31112 (2004).
[35] A. Cheng, M.L. Klein, C. Caccamo. Prediction of the phase diagram of rigid C_{60} molecules. *Phys. Rev. Lett.*, **71**(8), 1200 (1993).
[36] S. Brown, J. Cao, J.L. Musfeldt, N. Dragoe, F. Cimpoesu, *et al.* Search for microscopic evidence for molecular level negative thermal expansion in fullerenes. *Phys. Rev. B*, **42**, 125446 (2006).
[37] M.K. Balasubramanya, M.W. Roth, P.D. Tilton, B.A. Suchy. Molecular dynamics simulations of noble gas release from endohedral fullerenes due to cage disintegration, [Refer to eprint archive submission—M.K. Balasubramanya, M.W. Roth, P.D. Tilton, B.A. Suchy, arXiv:cond-mat/0607535(2006)]

Downloaded At: 17:47 14 January 2011